Localised Nonlinear Modes in the *PT*-Symmetric Double-Delta Well Gross-Pitaevskii Equation

I.V. Barashenkov and D.A. Zezyulin

Abstract We construct exact localised solutions of the *PT*-symmetric Gross-Pitaevskii equation with an attractive cubic nonlinearity. The trapping potential has the form of two δ-function wells, where one well loses particles while the other one is fed with atoms at an equal rate. The parameters of the constructed solutions are expressible in terms of the roots of a system of two transcendental algebraic equations. We also furnish a simple analytical treatment of the linear Schrödinger equation with the *PT*-symmetric double-δ potential.

1 Introduction

We consider the Gross-Pitaevskii equation,

$$i\,\Psi_t + \Psi_{xx} - V(x)\Psi + g|\Psi|^2\Psi = 0, \tag{1}$$

with $g \geq 0$ and the *PT*-symmetric potential

$$V(x) = U(x) + iW(x), \qquad U(-x) = U(x), \quad W(-x) = -W(x). \tag{2}$$

The system (1)–(2) was employed to model the dynamics of the self-gravitating boson condensate trapped in a confining potential $U(x)$. The imaginary coefficient

I.V. Barashenkov (✉)
National Institute for Theoretical Physics, Stellenbosch,
Western Cape, South Africa
e-mail: Igor.Barashenkov@uct.ac.za

I.V. Barashenkov
Department of Mathematics, University of Cape Town, Rondebosch 7701,
Cape Town, South Africa

D.A. Zezyulin
Centro de Física Teórica e Computacional and Departamento de Física,
Faculdade de Ciências da Universidade de Lisboa, Campo Grande, Edifício C8,
Lisboa, 1749-016 Lisbon, Portugal
e-mail: dzezyulin@fc.ul.pt

F. Bagarello et al. (eds.), *Non-Hermitian Hamiltonians in Quantum Physics*,
Springer Proceedings in Physics 184, DOI 10.1007/978-3-319-31356-6_8

iW accounts for the particle leakage—in the region where $W(x) < 0$—and the compensatory injection of atoms in the region where $W(x) > 0$ [1, 2].

The same equation was used to describe the stationary light beam propagation in the self-focusing Kerr medium. In the optical context, t stands for the scaled propagation distance while Ψ is the complex electric-field envelope. The real part of the potential (U) is associated with the refractive index guiding, while the imaginary part (W) gives the optical gain and loss distribution [3].

We are interested in localised solutions of this equation, that is, solutions with the asymptotic behaviour $\Psi(x,t) \to 0$ as $x \to \pm\infty$. We also require that

$$\int_{-\infty}^{\infty} |\Psi|^2 dx = 1. \tag{3}$$

In the context of leaking condensate with injection, the normalisation condition (3) implies that the total number of particles in the condensate is kept at a constant level.

In this study, we consider stationary solutions of the form $\Psi(x,t) = \psi(x)e^{i\kappa^2 t}$, where κ^2 is real and the spatial part of the eigenfunction obeys

$$-\psi_{xx} + V(x)\psi - g\psi|\psi|^2 = -\kappa^2\psi. \tag{4}$$

Assuming that the potential satisfies $V(x) \to 0$ as $x \to \pm\infty$, the coefficient κ^2 has to be taken positive. For definiteness, we choose the real quantity κ to be positive as well. Equation (4) will be solved under the normalisation constraint

$$\int_{-\infty}^{\infty} |\psi|^2 dx = 1, \tag{5}$$

stemming from the condition (3).

Our study will be confined to the PT-symmetric solutions of equation (4), that is, solutions satisfying

$$\psi(-x) = \psi^*(x). \tag{6}$$

Typically, stationary solutions supported by PT-symmetric potentials can be brought to the form (6) by a suitable constant phase shift.

With an eye to the forthcoming study of the jamming anomaly [4], we consider a PT-symmetric potential of the special form:

$$V(x) = -(1 - i\gamma)\delta(x + L/2) - (1 + i\gamma)\delta(x - L/2). \tag{7}$$

Here $\gamma \geq 0$ and $L > 0$. The $V(x)$ is an idealised potential consisting of two infinitely deep wells. The right-hand well is leaking particles, while its left-hand counterpart is injected with atoms at an equal constant rate γ.

Previous analyses of the double-delta cubic Gross-Pitaevskii equation focused mainly on the situation with no gain or loss—that is, on the potential (7) with $\gamma = 0$. Using a combination of analytical and numerical tools, Gaididei, Mingaleev and Christiansen [5] demonstrated the spontaneous breaking of the left-right symmetry by localised solutions. Subsequently, Jackson and Weinstein [6] performed geometric analysis of the symmetry breaking and classified the underlying bifurcations of stationary solutions. Besides the absence of gain and loss, the mathematical setting of [6] was different from our present problem in that the normalisation condition (3) was not imposed there.

Studies of the *PT*-symmetric model with $\gamma \neq 0$ were pioneered by Znojil and Jakubský who analysed the linear Schrödinger equation with point-like gain and loss (but no wells) on a finite interval [7, 8]. The double-well potential (7) was proposed by Uncu and Demiralp [9] whose paper also focussed on the linear equation—yet on the infinite line. Cartarius and Wunner [2, 10] considered both linear and nonlinear Gross-Pitaevskii model. The numerical study of [2, 10] identified a branch of localised nonlinear modes bifurcating from eigenfunctions of the linear operator in (4).

In this contribution, we get an analytical handle on the *PT*-symmetric double-δ problem, linear and, most importantly, nonlinear. In the linear situation (equation (4) with $g = 0$) we provide a mathematical interpretation and verification of the numerics reported in [2, 10]. In the nonlinear case ($g \neq 0$), the analytical consideration allows us to advance beyond the numerical conclusions of the previous authors. In particular, we demonstrate the existence of infinite families of localised solutions with multiple humps and dips between the two potential singularities.

2 Linear Schrödinger Equation with Complex Double-δ Well Potential

Relegating the analysis of the full nonlinear equation (4), (7) to the subsequent sections, here we consider its linear particular case ($g = 0$). The normalised eigenfunction pertaining to the eigenvalue $-\kappa^2$ is given by

$$\psi(x) = \begin{cases} \frac{e^{i\phi}+e^{\kappa L-i\phi}}{2\sqrt{N}} e^{\kappa x}, & x \leq -L/2; \\ \frac{\cosh(\kappa x+i\phi)}{\sqrt{N}}, & -L/2 \leq x \leq L/2; \\ \frac{e^{-i\phi}+e^{\kappa L+i\phi}}{2\sqrt{N}} e^{-\kappa x}, & x \geq L/2. \end{cases}$$

Here κ is a positive root of the transcendental equation [2, 9, 10]

$$e^{-2\kappa L} = \frac{\gamma^2 + (2\kappa - 1)^2}{\gamma^2 + 1}, \tag{8}$$

while ϕ and N are readily expressible through κ. The secular equation (8) was solved numerically in [2, 10]. Here, we analyse it without resorting to the help of computer.

To this end, we express γ as an explicit function of κ:

$$\gamma^2 = \frac{4\kappa(1-\kappa)}{1-e^{-2\kappa L}} - 1. \tag{9}$$

Instead of evaluating eigenvalues κ as the parameter $\gamma > 0$ is varied, we identify the range of positive κ where the function $\gamma^2(\kappa)$ is positive. We prove the following

Proposition 1 *Regardless of the value of L, there is a finite interval of κ where $\gamma^2 > 0$. When $L < 2$, the interval is $0 < \kappa < \kappa^{(b)}$, and when $L > 2$, the interval is $\kappa^{(a)} < \kappa < \kappa^{(b)}$. Here $\kappa^{(a)}$ and $\kappa^{(b)}$ are dependent on L, with $0 < \kappa^{(a)} < \kappa^{(b)} < 1$.*

Proof The inequality $\gamma^2 > 0$ amounts to $k_1 < \kappa < k_2$, where the endpoints of the interval (k_1, k_2) also depend on κ:

$$k_1(\kappa) = \frac{1-e^{-\kappa L}}{2}, \quad k_2(\kappa) = \frac{1+e^{-\kappa L}}{2}.$$

If $L < 2$, the quantity $k_1(\kappa)$ is smaller than κ for all $\kappa > 0$. If, on the other hand, $L > 2$, the graph of the function $y = k_1(\kappa)$ lies above $y = \kappa$ in the interval $0 \le \kappa < \kappa^{(a)}$ and below $y = \kappa$ in the interval $\kappa^{(a)} < \kappa < \infty$. Here $\kappa^{(a)} = \kappa^{(a)}(L)$ is the (unique) root of the equation $k_1(\kappa) = \kappa$.

On the other hand, the function $k_2(\kappa)$ is greater than κ when $0 < \kappa < \kappa^{(b)}$ and smaller than κ when $\kappa > \kappa^{(b)}$. Here $\kappa^{(b)} = \kappa^{(b)}(L)$ is the root of the equation $k_2(\kappa) = \kappa$. (There is a unique root for all $L > 0$.)

Note that in the range of the L values where the root $\kappa^{(a)}$ exists—that is, in the region $L > 2$—we have $\kappa^{(a)} < \kappa^{(b)}$. Since $\kappa_2(1) < 1$, we have $\kappa^{(b)} < 1$. □

Our next result concerns the number of eigenvalues arising for various γ. Again, instead of counting branches of the function $\kappa(\gamma)$, we identify regions of monotonicity of the inverse function, $\gamma(\kappa)$. These are separated by the points of local extrema (stationary points).

Proposition 2 *When $L < 1$, the function $\gamma(\kappa)$ is monotonically decreasing as κ changes from 0 to $\kappa^{(b)}$, with $\kappa^{(b)}$ defined above. When $L > 1$, the function $\gamma(\kappa)$ has a single local maximum at $\kappa = \kappa_c$ (where $\kappa_c < \kappa^{(b)}$).*

Proof Stationary points of the function $\gamma^2(\kappa)$ are given by zeros of

$$\frac{d\gamma^2}{d\kappa} = \frac{(1-2\kappa)}{2\kappa L \sinh^2(L\kappa)} [f(\kappa) - g(\kappa)], \tag{10}$$

where

$$f = \frac{e^{2L\kappa}-1}{2L\kappa}, \quad g = \frac{1-\kappa}{1-2\kappa}.$$

We consider (10) for $0 < \kappa < 1$. (Note that $\kappa = 1/2$ is not a zero of $d\gamma^2/d\kappa$.) When $1/2 < \kappa < 1$, the function g is strictly negative; hence stationary points may only lie in the interval $0 < \kappa < 1/2$.

Assume, first, that $L < 1$ and expand $f(\kappa)$ and $g(\kappa)$ in powers of κ:

$$f = 1 + \sum_{n=1}^{\infty} f_n \kappa^n, \quad f_n = \frac{(2L)^n}{(n+1)!} \tag{11}$$

$$g = 1 + \sum_{n=1}^{\infty} g_n \kappa^n, \quad g_n = 2^{n-1}. \tag{12}$$

The series (11) converges in the entire complex plane of κ while the series (12) converges in the disc $|\kappa| < 1/2$. Noting that $f_n < g_n$ for all n, we conclude that $f(\kappa) < g(\kappa)$ for all $0 < \kappa < 1/2$. Equation (10) implies then that for any $L < 1$, the function $\gamma^2(\kappa)$ decreases monotonically as κ changes from 0 to 1.

Let now $L > 1$. The values of f and g at the origin are equal while their slopes are not:

$$\left.\frac{df}{d\kappa}\right|_{\kappa=0} = L, \quad \left.\frac{dg}{d\kappa}\right|_{\kappa=0} = 1.$$

Consequently, the graph of $f(\kappa)$ lies above the graph of $g(\kappa)$ as long as κ remains sufficiently close to the origin. At the opposite end of the interval, that is, in the vicinity of $\kappa = 1/2$, the graph of $g(\kappa)$ lies above $f(\kappa)$. Therefore the equation $f(\kappa) = g(\kappa)$ has (at least one) root κ_c in the interval $0 < \kappa < 1/2$. This root emerges from the point $\kappa = 0$ as soon as L becomes greater than 1.

To show that no additional stationary points can emerge as L is further increased, assume the contrary—assume that a pair of stationary points is born as L passes through a critical value L_* (where $L_* > 1$). At the bifurcation value $L = L_*$, the newborn stationary points are equal; we denote them κ_*. When $L = L_*$, the equality

$$\left.\frac{df}{d\kappa}\right|_{\kappa=\kappa_*} = \left.\frac{dg}{d\kappa}\right|_{\kappa=\kappa_*} \tag{13}$$

should be fulfilled along with

$$f(\kappa_*) = g(\kappa_*). \tag{14}$$

Solving the system (13), (14) yields $L_* = (1 - 2\kappa_*)^{-1}$. This can be written as

$$L_* = 1 + q, \tag{15}$$

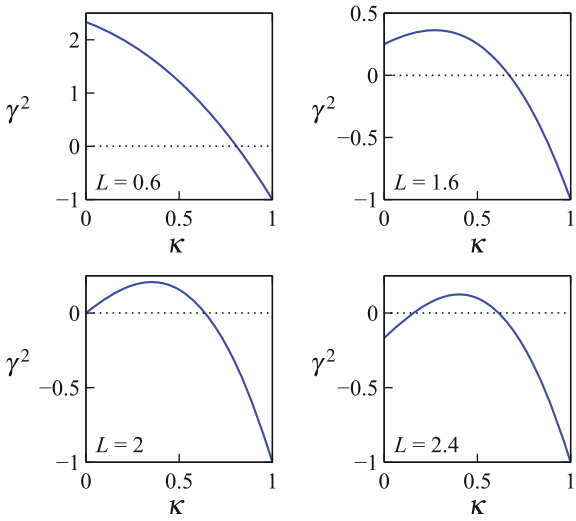

Fig. 1 The function (9) plotted for several representative values of L. In the interval of κ where $\gamma^2 \geq 0$, the function gives the square of the gain-loss coefficient. The inverse function $\kappa(\gamma^2)$ is obtained simply by flipping the part of the graph with $\gamma^2 \geq 0$ about the $\gamma^2 = \kappa$ line (see Fig. 2)

where we have defined $q = 2\kappa_* L_*$. Making use of (15), equation (14) becomes

$$\frac{e^q - 1}{q} = 1 + \frac{q}{2}.$$

Expanding the left-hand side in powers of q one can readily check that it is greater than the right-hand side for any $q > 0$; hence the above equality can never be satisfied. This proves that the stationary point κ_c of the function $\gamma^2(\kappa)$ is single.

Since $d\gamma^2/d\kappa|_{\kappa=0} > 0$, the stationary point κ_c is a maximum. □

The above propositions are illustrated by Fig. 1 which shows $\gamma^2(\kappa)$ with $L < 1$ (a); $1 < L < 2$ (b); $L = 2$ (c), and $L > 2$ (d).

Our conclusions are sufficient to determine the shape of the inverse function, $\kappa(\gamma)$. When $L < 1$, there is a single positive branch of $\kappa\ (\gamma)$ which decays, monotonically, as γ is increased from zero to γ_0 (Fig. 2a). As γ reaches γ_0, the quantity κ drops to zero and the eigenvalue $-\kappa^2$ collides with the continuous spectrum. Since $\gamma^2(0) = 2/L - 1$, we can obtain the critical value of γ exactly: $\gamma_0 = \gamma(0) = \sqrt{2/L - 1}$.

When L is taken between 1 and 2, the function $\kappa\ (\gamma)$ has two branches (Fig. 2b). Along the monotonically decreasing branch, κ drops from $\kappa^{(b)}$ to κ_c as γ is raised from 0 to γ_c. In addition, there is a monotonically increasing branch with $\gamma_0 < \gamma < \gamma_c$. Here, κ grows from 0 to κ_c as γ is increased from γ_0 to γ_c. The two eigenvalues merge and become complex as γ is raised through γ_c.

Finally, when $L \geq 2$, the monotonically decreasing and increasing branch of $\kappa(\gamma)$ exist over the same interval $0 < \gamma < \gamma_c$ (Fig. 2c, d). As γ grows from 0 to γ_c, one branch of κ grows from $\kappa^{(a)}$ to κ_c whereas the other one decreases from $\kappa^{(b)}$ to κ_c.

These conclusions are in agreement with the numerical results of [2, 10].

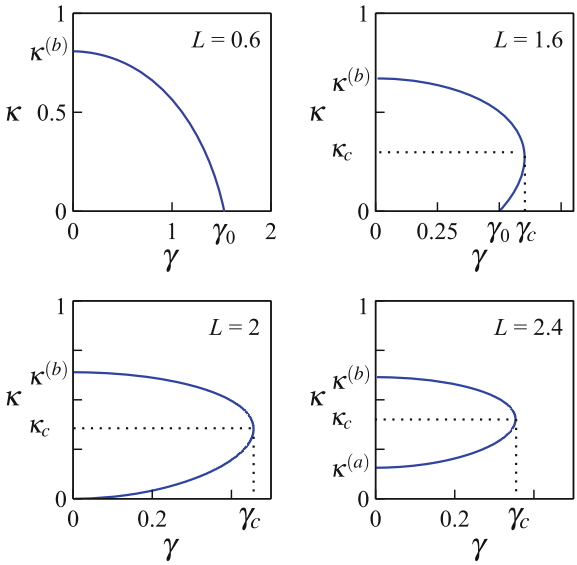

Fig. 2 Positive roots of (8) versus the gain-loss coefficient γ, for several representative values of L

3 *PT*-Symmetric Gross-Pitaevskii Equation with Variable-Depth Wells

Proceeding to the nonlinear situation ($g \neq 0$), it is convenient to transform the stationary equation (4) to

$$\varphi_{\tau\tau} + \lambda\,[\delta(\tau + T) + \delta(\tau - T)]\,\varphi - i\eta[\delta(\tau + T) - \delta(\tau - T)]\varphi + 2\varphi|\varphi|^2 = \varphi, \tag{16}$$

with

$$\tau = \kappa x, \quad T = \kappa\frac{L}{2}, \quad \varphi = \sqrt{\frac{g}{2}}\frac{\psi}{\kappa}, \quad \lambda = \frac{1}{\kappa}, \quad \eta = \frac{\gamma}{\kappa}.$$

Here $\eta \geq 0$, $\lambda > 0$, and $T > 0$. In equation (16) the chemical potential has been normalised to unity at the expense of making the well depths, λ, variable. The normalisation constraint (5) acquires the form

$$\int_{-\infty}^{\infty} |\varphi|^2 d\tau = \frac{\lambda}{2}g, \tag{17}$$

while the symmetry condition (6) translates into

$$\varphi^*(\tau) = \varphi(-\tau). \tag{18}$$

Consider a solution $\varphi(\tau)$ of the equation (16) and denote $N = \int |\varphi|^2 d\tau$ the corresponding number of particles. The number of particles is a function of λ, η and T: $N = N(\lambda, \eta, T)$. Setting g to a particular value, the constraint (17) defines a two-dimensional surface in the (λ, η, T) space:

$$\frac{1}{\lambda} N(\lambda, \eta, T) = \frac{g}{2}.$$

For any fixed L, the "nonlinear eigenvalue" $\kappa = \lambda^{-1}$ becomes an (implicit) function of γ:

$$\kappa N\left(\frac{1}{\kappa}, \frac{\gamma}{\kappa}, \frac{\kappa L}{2}\right) = \frac{g}{2}.$$

The purpose of our study is to construct the solution $\varphi(\tau)$ and determine this function.

It is fitting to note here that the equation (4) with $g = 0$ can also be transformed to the form (16)—where one just needs to drop the cubic term. In this case, the number of particles is not fixed though; that is, the constraint (17) does not need to be satisfied. The relation between κ and γ—equation (8)—arises as a secular equation for an eigenvalue problem.

4 Particle Moving in a Mexican-Hat Potential

In the external region $|\tau| \geq T$, the PT-symmetric solutions with the boundary conditions $\varphi(\pm\infty) = 0$ have the form

$$\begin{aligned} \varphi(\tau) &= e^{-i\chi} \operatorname{sech}(\tau + \mu), \quad \tau \leq -T; \\ \varphi(\tau) &= e^{i\chi} \operatorname{sech}(\tau - \mu), \quad \tau \geq T. \end{aligned} \tag{19}$$

Here μ is an arbitrary real value, positive or negative, determining the amplitude of φ, and χ is an arbitrary real phase. The solution $\varphi(\tau)$ in the internal region $|\tau| \leq T$ will be matched to the values of (19) at the endpoints $\tau = \pm T$:

$$\varphi(\pm T) = e^{\pm i\chi} \operatorname{sech}(\mu - T). \tag{20}$$

Integrating (16) across the singularities and using (19) once again, we obtain the matching conditions for the derivatives as well:

$$\begin{aligned} \dot{\varphi}|_{\tau=T-0} &= e^{i\chi} \operatorname{sech}(\mu - T)[i\eta + \lambda + \tanh(\mu - T)], \\ \dot{\varphi}|_{\tau=-T+0} &= e^{-i\chi} \operatorname{sech}(\mu - T)[i\eta - \lambda - \tanh(\mu - T)]. \end{aligned} \tag{21}$$

Here the overdot stands for the differentiation with respect to τ.

To construct the solution between $-T$ and T it is convenient to interpret the modulus and the phase of φ as polar coordinates of a particle on the plane,

$$\varphi = re^{i\theta},$$

and the coordinate τ as time. The newtonian particle moves in the radial-symmetric mexican hat-shaped potential $U(r) = \frac{1}{2}(r^4 - r^2)$. Hence the angular momentum

$$\ell = \dot{\theta} r^2 \tag{22}$$

and the energy

$$\mathscr{E} = \frac{\dot{r}^2}{2} + U_{\text{eff}}(r), \quad U_{\text{eff}} = \frac{\ell^2}{2r^2} + \frac{r^4 - r^2}{2} \tag{23}$$

are conserved. The effective potential for the radial motion is shown in Fig. 3a.

The particle starts its motion at time $\tau = -T$ and ends at $\tau = T$. The boundary conditions follow from (20) and (21):

$$r(\pm T) = \operatorname{sech}(\mu - T), \tag{24}$$

$$\dot{r}(-T) = -\dot{r}(T) = -(\lambda + \xi)\operatorname{sech}(\mu - T), \tag{25}$$

$$\theta(\pm T) = \pm\chi, \tag{26}$$

$$\dot{\theta}(\pm T) = \eta, \tag{27}$$

where

$$\xi = \tanh(\mu - T).$$

The parameter ξ satisfying $\lambda + \xi > 0$ requires a negative initial velocity, $\dot{r}(-T) < 0$, and $\lambda + \xi < 0$ corresponds to an outward initial motion: $\dot{r}(-T) > 0$.

Equations (22) and (27) imply that the conserved angular momentum has a positive value:

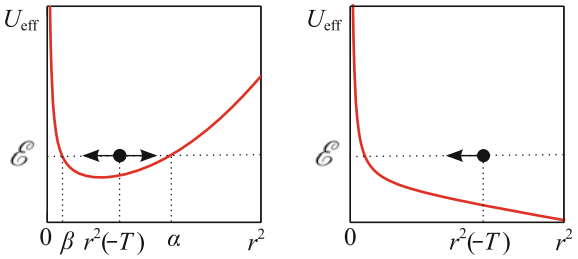

Fig. 3 The *left panel* shows $U_{\text{eff}}(r)$, the effective potential of radial motion defined in (23). *Two arrows* indicate two possible directions of motion of the fictitious particle. Whether the particle starts with a positive or negative radial velocity, it will run into a turning point. Dropping the quartic term from (23) gives the effective potential for the linear equation (*right panel*). This time the turning point will only be run into if $\dot{r}(-T) < 0$

$$\ell = \eta\,\mathrm{sech}^2(\mu - T) \tag{28}$$

and so θ grows as τ varies from $-T$ to T. (Hence $\chi > 0$.) The energy of the particle is found by substituting (24)–(25) in (23):

$$\mathscr{E} = \frac{1}{2}(1-\xi^2)\left[(\lambda+\xi)^2 - \xi^2 + \eta^2\right]. \tag{29}$$

Since the energy (23) includes the square of $\dot{r}$ but not $\dot{r}$ itself, the information about the initial direction of motion becomes lost in the expression (29). In fact, by using the value of energy instead of the boundary condition (25) we are acquiring spurious solutions. These solutions have the wrong sign of $\dot{r}(\tau)$ as $\tau \to -T+0$ and do not satisfy (25). Fortunately we remember that the sign of $\dot{r}|_{\tau\to -T+0}$ should be opposite to that of $\lambda+\xi$. This simple rule will be used to filter out the spurious roots in Sect. 7.

The radial trajectory $r(\tau)$ for a PT-symmetric solution satisfying (18) should be described by an even function and the trajectory should have a turning point at $\tau = 0$: $\dot{r}(0) = 0$. The separable equation (23) has two even solutions,

$$r_A^2(\tau) = (\alpha-\beta)\mathrm{cn}^2\left(\sqrt{2\alpha+\beta-1}\,\tau, k\right) + \beta \tag{30}$$

and

$$r_B^2(\tau) = (\alpha-\beta)\mathrm{cn}^2\left(K - \sqrt{2\alpha+\beta-1}\,\tau, k\right) + \beta. \tag{31}$$

The Jacobi-function solutions (30) and (31) are parametrised by two parameters, α and β, where $\alpha \geq \beta \geq 0$ and $\alpha+\beta > 1$. These are related to ℓ and $\mathscr{E}$ via

$$\ell^2 = \alpha\beta(\alpha+\beta-1), \tag{32}$$

$$2\mathscr{E} = (\alpha+\beta)(\alpha+\beta-1) - \alpha\beta. \tag{33}$$

The elliptic modulus k is given by

$$k^2 = \frac{\alpha-\beta}{2\alpha+\beta-1},$$

and $K(k)$ in (31) is the complete elliptic integral of the first kind. Eliminating ℓ between (28) and (32), and $\mathscr{E}$ between (29) and (33) we get

$$\eta^2(1-\xi^2)^2 = \alpha\beta(\alpha+\beta-1), \tag{34}$$

$$(1-\xi^2)(\lambda^2+\eta^2+2\lambda\xi) = (\alpha+\beta)(\alpha+\beta-1) - \alpha\beta. \tag{35}$$

The solution r_A is maximum-centred and r_B is minimum-centred (see Fig. 4).

For the purposes of our study, it is convenient to have a relation between α, β, and ξ not involving the gain-loss parameter. Eliminating η^2 between (34) and (35)

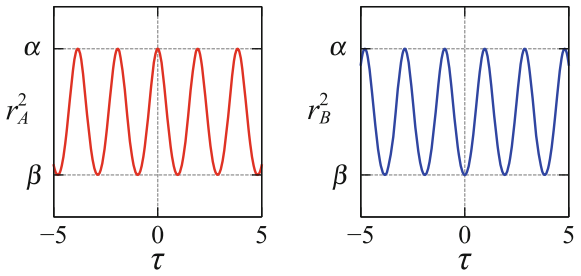

Fig. 4 Two even solutions of equation (23). **a** The maximum-centred solution, equation (30). **b** The minimum-centred solution, equation (31). In both panels $\alpha = 2$ and $\beta = 0.5$

we obtain

$$(\lambda + \xi)^2 = S^2, \tag{36}$$

where

$$S^2 = \frac{(\alpha+\beta)(\alpha+\beta-1)-\alpha\beta}{1-\xi^2} - \frac{\alpha\beta(\alpha+\beta-1)}{(1-\xi^2)^2} + \xi^2. \tag{37}$$

The structural relation (36)–(37) will prove useful in what follows.

5 Boundary Conditions and Normalisation Constraint

The boundary conditions (24) give a transcendental equation

$$\beta + (\alpha - \beta)\mathrm{cn}^2\,(y, k) = 1 - \xi^2, \tag{38a}$$

for the r_A and

$$\beta + (\alpha - \beta)\mathrm{cn}^2\,(K - y, k) = 1 - \xi^2 \tag{38b}$$

for the r_B solution. Here

$$y = \sqrt{2\alpha + \beta - 1}\,T.$$

Note that there is a simple correspondence between equations (38a) and (38b). Namely, if we assume that α, β and ξ in (38a) and (38b) are given, and denote $\widetilde{y}$ the value of y satisfying (38b), then $y = K - \widetilde{y}$ will satisfy (38a).

The linear ($g = 0$) Schrödinger equation (4) with the potential (7) corresponds to the newtonian particle moving in the effective potential without the quartic barrier at large r. In this case the particle can only run into a turning point if $\dot{r}(-T) < 0$ (see Fig. 3b). On the other hand, when the quartic barrier is present, the particle will turn no matter whether $\dot{r}(-T)$ is negative or positive (Fig. 3a).

Consider, first, the solution $r_A(\tau)$ and assume that $\dot{r}(-T) > 0$. The simplest trajectory satisfying the boundary conditions (24)–(25) describes the particle starting with a positive radial velocity at $\tau = -T$, reaching the maximum $r^2 = \alpha$ at $\tau = 0$ and returning to the starting point at $\tau = T$. We use T_0 to denote the corresponding

return time, T. Coexisting with this solution are longer trajectories that reach the maximum $r^2 = \alpha$ not once but $2n + 1$ times ($n \geq 1$), namely, at $\tau = 2m\Theta$, where

$$\Theta = \frac{K(k)}{\sqrt{2\alpha + \beta - 1}} \tag{39}$$

is the half-period of the function $\mathrm{cn}^2(\sqrt{2\alpha + \beta - 1}\tau, k)$ and $m = 0, \pm 1, \pm 2, ..., \pm n$. These trajectories have the same values of α and β (the same apogee and perigee) but different return times, $T = T_0 + 2n\Theta$. Since the trajectory reaches its apogee $2n + 1$ times and pays $2n$ visits to its minimum value of $r^2 = \beta$, we are referring to these solutions as $(2n + 1)$-hump, $2n$-dip nonlinear modes.

In contrast to these, the r_A solution with $\dot{r}(-T) < 0$ will be visiting its minimum $2n$ times ($n \geq 1$), at $\tau = (1 - 2n)\Theta$, ...$(2n - 1)\Theta$, but will only pay $2n - 1$ visits to its maximum. These trajectories will be classified as $2n$-dip, $(2n - 1)$-hump modes. The corresponding return times are $T = 2n\Theta - T_0$.

Turning to the minimum-centred solutions, we consider trajectories with $\dot{r}(-T) < 0$ first. The simplest r_B solution describes the particle starting with a negative velocity at $\tau = -T$, reaching its perigee $r^2 = \beta$ at $\tau = 0$ and returning to the starting point at $\tau = T$, where $T = \Theta - T_0$ and T_0 was introduced above. The r_B solutions with more bounces visit the minimum r not once but $2n + 1$ times ($n \geq 1$), at $\tau = 2m\Theta$, $m = 0, \pm 1, ..., \pm n$. The corresponding return time is $T = (2n + 1)\Theta - T_0$. With their $2n + 1$ local minima and $2n$ maxima, these solutions are referred to as the $(2n + 1)$-dip, $2n$-hump nonlinear modes.

Finally, the r_B solution with $\dot{r}(-T) > 0$ reaches its apogee $2n$ times ($n \geq 1$), that is, at $\tau = (2m + 1)\Theta$, with $m = -n - 1, ..., n$. The return time is $T = T_0 + (2n - 1)\Theta$. The trajectory pays $2n - 1$ visits to its minimum value of $r^2 = \beta$; hence we classify this solution as the $2n$ hump, $(2n - 1)$-dip modes.

For the fixed α and β, the return time T_0 is given by the smallest positive root of (38a). (Note that $T_0 < \Theta$.) Other roots of this equation are $T_0 + 2\Theta$, $T_0 + 4\Theta$, ..., and $2\Theta - T_0$, $4\Theta - T_0$, ... On the other hand, the smallest positive root of (38b) is $\Theta - T_0$, with other roots being $3\Theta - T_0$, $5\Theta - T_0$, ..., and $T_0 + \Theta$, $T_0 + 3\Theta$, ...

The normalised return time

$$\frac{T}{\Theta} = \frac{y}{K(k)} \tag{40}$$

provides a simple tool for the identification of the nonlinear mode. Indeed, an r_A solution with T/Θ between $2n$ and $2n + 1$ has $2n + 1$ humps, $2n$ dips and $\dot{r}(-T) > 0$. On the other hand, an r_A solution with T/Θ between $2n - 1$ and $2n$ has $2n$ dips, $2n - 1$ humps and $\dot{r}(-T) < 0$. Similarly, an r_B solution will have $2n$ humps, $2n - 1$ dips, and $\dot{r}(-T) > 0$—if T/Θ lies between $2n - 1$ and $2n$, or $2n + 1$ dips, $2n$ humps, and $\dot{r}(-T) < 0$—if T/Θ is between $2n$ and $2n + 1$.

Evaluating the number of particles

$$N = \int_{-\infty}^{-T} \operatorname{sech}^2(\tau + \mu)d\tau + \int_{-T}^{T} r_A^2 d\tau + \int_{T}^{\infty} \operatorname{sech}^2(\tau - \mu)d\tau$$

and substituting in the normalisation constraint (17), the constraint is transformed into

$$\zeta_A(\alpha, \beta, y, \lambda) = \xi, \tag{41}$$

where the function ζ_A is defined by

$$\zeta_A = \frac{\alpha + \beta - 1}{\sqrt{2\alpha + \beta - 1}} y - 1 + \frac{g}{4}\lambda - \sqrt{2\alpha + \beta - 1}\, E\left[\operatorname{am}(y)\right]. \tag{42}$$

Here $E[\operatorname{am}(y)] = E[\operatorname{am}(y), k]$ is the incomplete elliptic integral of the second kind,

$$E[\operatorname{am}(y), k] = \int_0^{\operatorname{am}(y)} \sqrt{1 - k^2 \sin^2\theta}\, d\theta = \int_0^{y} \operatorname{dn}^2(w, k) dw,$$

and $\operatorname{am}(y)$ is the elliptic amplitude. (To simplify the notation, we omit the dependence on the elliptic modulus k in (42).)

A similar procedure involving the solution r_B yields

$$\zeta_B(\alpha, \beta, y, \lambda) = \xi, \tag{43}$$

where we have introduced

$$\zeta_B = \frac{\alpha + \beta - 1}{\sqrt{2\alpha + \beta - 1}} y - 1 + \frac{g}{4}\lambda - \sqrt{2\alpha + \beta - 1}\left\{E\left(\frac{\pi}{2}\right) - E\left[\operatorname{am}(K - y)\right]\right\}. \tag{44}$$

Here $E(\pi/2) = E(\pi/2, k)$ is the complete elliptic integral of the second kind.

Note that unlike the pair of equations (38a) and (38b), the normalisation constraints (41) and (43) are not related by the transformation $y = K - \widetilde{y}$. Therefore, the solution of the system (38b)+(43) cannot be reduced to solving (38a)+(41). The "r_A" and "r_B" systems have to be considered independently.

6 Reduction to the Linear Schrödinger Equation

Before proceeding to the analysis of the systems (38a)+(41) and (38b)+(43), it is instructive to verify that the transcendental equation (8) for the linear Gross-Pitaevskii equation is recovered as the $g \to 0$ limit of (38b).

Assume that κ is fixed and g is varied in the stationary Gross-Pitaevskii equation (4). When g is small, the solution of (4) bifurcating from the solution of the corresponding *linear* Schrödinger equation remains of order 1. The corresponding solution φ of equation (16) will then have to be of order $g^{1/2}$. This means, in particular, that for all $|\tau| \geq T$, the "outer" solution (19) will have to approach zero as $g \to 0$. In order to have

$$\int_T^\infty \mathrm{sech}^2(\tau - \mu) d\tau \to 0 \quad \text{as } g \to 0,$$

one has to require that $\tanh(\mu - T) \to -1$ as $g \to 0$. Defining σ by

$$\mathrm{sech}^2(\mu - T) = \sigma^2 g, \quad \sigma = O(1), \tag{45}$$

the quantity $\xi = \tanh(\mu - T)$ will have the following asymptotic behaviour:

$$\xi = -1 + \frac{\sigma^2}{2} g + O(g^2).$$

Letting

$$\alpha = 1 + \mathscr{A}_1 g + \mathscr{A}_2 g^2 + \cdots, \quad \beta = \mathscr{B}_1 g + \mathscr{B}_2 g^2 + \cdots$$

and substituting these expansions in (34) and (35) gives

$$\mathscr{A}_1 = A\sigma^2, \quad \mathscr{B}_1 = B\sigma^2,$$

where

$$A = \lambda^2 - 2\lambda + \eta^2, \quad B = -\frac{1}{2} A + \frac{1}{2}\sqrt{A^2 + 4\eta^2}. \tag{46}$$

Turning to the transcendental equation (38b), we note that the elliptic modulus of the Jacobi cosine tends to 1 as $g \to 0$:

$$k^2 = 1 - (\mathscr{A}_1 + 2\mathscr{B}_1) g + \cdots$$

In this limit, the elliptic function approaches a hyperbolic sine:

$$\mathrm{cn}(K - y, k) = k' \sinh y + O(k'^3), \quad k'^2 = 1 - k^2.$$

In equation (38b), $y = \sqrt{2\alpha + \beta - 1}\, T$. With $\sqrt{2\alpha + \beta - 1} = 1 + O(g)$, the transcendental equation reduces to

$$B + (A + 2B) \sinh^2 T = 1. \tag{47}$$

Substituting for A and B from (46), equation (47) gives

$$e^{-4T} = \frac{(\lambda - 2)^2 + \eta^2}{\lambda^2 + \eta^2}. \tag{48}$$

Transforming to $\gamma = \eta/\lambda$, $\kappa = 1/\lambda$ and $L = 2\lambda T$, we recover the transcendental equation (8).

Finally, we consider the normalisation constraint (43). As $k \to 1$, the elliptic integral of the second kind has the following asymptotic behaviour:

$$E\left(\frac{\pi}{2}\right) - E\left[\mathrm{am}(K - y)\right] = k'^2 \int_0^y \frac{du}{\mathrm{dn}^2(u, k)} = \frac{k'^2}{2}\left(y + \frac{\sinh 2y}{2}\right) + O\left(k'^4\right).$$

Making use of this expansion, we reduce equation (43) to

$$2 - 2AT + \sqrt{A^2 + 4\eta^2}\sinh(2T) = \frac{\lambda}{\sigma^2}. \tag{49}$$

Given λ, η and T, equation (49) furnishes the coefficient σ in the relation (45). The relation (45), in turn, determines the amplitude of the solution φ corresponding to the nonlinearity parameter g.

7 Transcendental Equations

In this section we assume that L, the distance between the potential wells in the original Gross-Pitaevskii equation (4), and g, the coefficient of the nonlinearity, are fixed. On the other hand, the gain-loss coefficient γ and the "nonlinear eigenvalue" κ (and hence the scaling factor $\lambda = \kappa^{-1}$, the scaled gain-loss $\eta = \gamma\kappa^{-1}$, and the dimensionless well-separation distance $2T = \kappa L$) are allowed to vary. The parameter ξ—the parameter defining the amplitude of the nonlinear mode—has not been fixed either.

Substituting ξ from the normalisation constraint (41) to the boundary condition (38a) we obtain a transcendental equation

$$\zeta_A^2 + \beta + (\alpha - \beta)\mathrm{cn}^2 y - 1 = 0 \tag{50a}$$

for the parameters of the r_A solution. In a similar way, substituting from (43) to (38b) we obtain an equation

$$\zeta_B^2 + \beta + (\alpha - \beta)\mathrm{cn}^2\left(K - y\right) - 1 = 0 \tag{50b}$$

for the solution r_B. Note that the functions ζ_A and ζ_B, defined in (42) and (44), depend on λ as a parameter.

Substituting ξ from the constraint (41) to the structural relation (36) gives another transcendental equation for the maximum-centred nonlinear mode:

$$(\lambda + \zeta_A)^2 - S_A^2 = 0. \tag{51a}$$

Here we are using a new notation S_A for the combination that was previously denoted S and given by (37). In a similar way, substituting ξ from (43) to (36) gives an equation for the minimum-centred (the r_B) solution:

$$(\lambda + \zeta_B)^2 - S_B^2 = 0, \tag{51b}$$

where the same combination S (defined in (37)) has been renamed S_B. (We are using two different notations for the same combination in order to be able to set the variable S to two different values later.) Like equations (50a) and (50b) before, equations (51a) and (51b) include λ as a parameter.

Eliminating $1 - \xi^2$ from the expression (37) by means of the boundary condition (38a), we specify S_A:

$$S_A^2 = \frac{(\alpha+\beta)(\alpha+\beta-1)-\alpha\beta}{\beta+(\alpha-\beta)\mathrm{cn}^2 y} - \frac{\alpha\beta(\alpha+\beta-1)}{\left[\beta+(\alpha-\beta)\mathrm{cn}^2 y\right]^2} + 1 - \beta - (\alpha-\beta)\mathrm{cn}^2 y. \tag{52a}$$

In order to specify S_B, we use the boundary condition (38b) instead:

$$S_B^2 = \frac{(\alpha+\beta)(\alpha+\beta-1)-\alpha\beta}{\beta+(\alpha-\beta)\mathrm{cn}^2\,(K-y)} - \frac{\alpha\beta(\alpha+\beta-1)}{\left[\beta+(\alpha-\beta)\mathrm{cn}^2\,(K-y)\right]^2} + 1 - \beta - (\alpha-\beta)\mathrm{cn}^2\,(K-y)\,. \tag{52b}$$

The system (50a), (51a) with ζ_A as in (42) and S_A as in (52a), is a system of two equations for two parameters of the solution r_A (the "A-system"). For the given L, g and λ, the A-system has one or several roots (α_n, β_n).

Not all roots define the Gross-Pitaevskii solitons though; some roots are spurious. To filter the spurious roots out, we use the simple rule formulated in Sect. 4. First, we calculate the normalised return time (40) and establish whether $2n < T/\Theta < 2n+1$ or $2n-1 < T/\Theta < 2n$ for some natural n. The former situation corresponds to $\dot{r}(-T) > 0$ and the latter to $\dot{r}(-T) < 0$. Evaluating the amplitude parameter ξ by means of (42), we then discard the roots with the sign of $\lambda + \xi$ coincident with the sign of $\dot{r}(-T)$.

Having thus validated the genuine roots for a range of λ values, we can use (38a) to express $1 - \xi^2$ through $\alpha(\lambda)$ and $\beta(\lambda)$, and then employ equation (34) to obtain $\eta(\lambda)$. Transforming from λ and η to $\kappa = 1/\lambda$ and $\gamma = \eta/\lambda$, we arrive at

$$\gamma_A(\kappa) = \frac{\sqrt{\alpha\beta(\alpha+\beta-1)}\kappa}{\beta + (\alpha-\beta)\mathrm{cn}^2\left(\sqrt{2\alpha+\beta-1}\kappa L/2\right)}. \tag{53a}$$

The transcendental system (50b), (51b), (44), (52b) (the "B-system") is not equivalent to the A-system and has to be solved independently. Having determined the roots $\alpha(\lambda)$, $\beta(\lambda)$ and validated them in the same way as we did with the A-roots before, we obtain an analogue of the formula (53a):

$$\gamma_B(\kappa) = \frac{\sqrt{\alpha\beta(\alpha+\beta-1)}\kappa}{\beta + (\alpha-\beta)\mathrm{cn}^2\left(K - \sqrt{2\alpha+\beta-1}\kappa L/2\right)}. \tag{53b}$$

The curve $\gamma(\kappa)$—or, equivalently, $\kappa(\gamma)$—will constitute the central result of our analysis. Each root (α_n, β_n) of the A- or B-system will contribute a branch to this curve. Before presenting the $\kappa(\gamma)$ relationships for various L and g, we note a useful symmetry of the A- and B-systems.

8 The Dip- and Hump-Adding Transformation

Consider the r_A solution and assume (α, β) is a root of the system (50a), (51a), (42), (52a) with parameters g, T and λ. The A-system with shifted parameters

$$\tilde{T} = T + 2\Theta, \quad \tilde{\lambda} = \lambda, \quad \tilde{g} = g + \Delta g,$$
$$\Delta g = \frac{8}{\lambda}\left[\sqrt{2\alpha+\beta-1}E - \frac{\alpha+\beta-1}{\sqrt{2\alpha+\beta-1}}K\right], \tag{54}$$

will have the same root (α, β). Here Θ is given by (39), while $K = K(k)$ and $E = E(k)$ are the complete elliptic integrals of the first and second kind, respectively.

The mapping (54) adds two units to the normalised return time T/Θ: $T/\Theta \to T/\Theta + 2$. Therefore (54) adds two humps and two dips to the A-mode with $2n$ dips and $2n \pm 1$ humps. Note that the expression in the square brackets in (54) is equal to $\int_0^\Theta r_A^2 d\tau$; hence $\Delta g > 0$ for any α and β. Therefore the map generates an infinite sequence of nonlinearity strengths g, $g + \Delta g$, $g + 2\Delta g$, ... supporting hump-centred nonlinear modes with an increasing number of lateral crests.

Turning to the B-solution and the system (50b), (51b), (44), (52b), the same mapping (54) transforms this system into itself. As a result of the application of the mapping (54), the B-solution with $2n$ humps and $2n \pm 1$ dips acquires two new humps and two new dips. The expression in the square brackets in (54) equals $\int_0^\Theta r_B^2 d\tau$; hence we have $\Delta g > 0$ in the case of the B solution as well. As with the A-solution before, the map (54) generates an infinite sequence of multicrest (yet dip-centred) modes.

9 *PT*-Symmetric Localised Nonlinear Modes

The A- and B-system of two transcendental equations were solved numerically. We employed a path-following algorithm with a newtonian iteration to obtain the root (α, β) as κ was varied with g and L fixed. The initial guess for the continuation process was provided either by the analysis of intersecting graphs of two simultaneous equations on the (α, β)-plane, or by transplanting a known root to a different set of g and L by means of the mapping (54).

Figure 5a traces a branch of the B-modes on the (γ, κ)-plane. Here, the parameters ($L = 2.2$ and $g = 1$) correspond to Fig. 1a in [2]. These are nonlinear modes with exactly one dip—at $x = 0$. The spatial structure of the mode is illustrated by Fig. 6a.

As it was established numerically in [2] and corroborated analytically in Sect. 6, the modes making up this branch are nonlinear deformations of the eigenfunctions of the linear Schrödinger equation (equation (4) with $g = 0$). This kinship is clearly visible in Fig. 6a where the nonlinear ($g = 1$) mode is plotted next to the normalized linear ($g = 0$) eigenfunction with the same value of γ.

In contrast to the above B branch, the A-modes exist only when g exceeds a certain finite threshold; these have no relation to the $g = 0$ eigenfunctions. A single-humped A-mode is exemplified by Fig. 6b, with the corresponding $\kappa(\gamma)$ branch appearing in Fig. 5b.

Finally, the bottom panels of Figs. 5 and 6 correspond to nonlinear modes with multiple humps and dips. The $\kappa(\gamma)$ curve in Fig. 5c pertains to a B-mode with three dips and two humps between the potential wells. This branch results by the κ-continuation from a root (α_0, β_0) of the B-system with κ equal to some κ_0 and

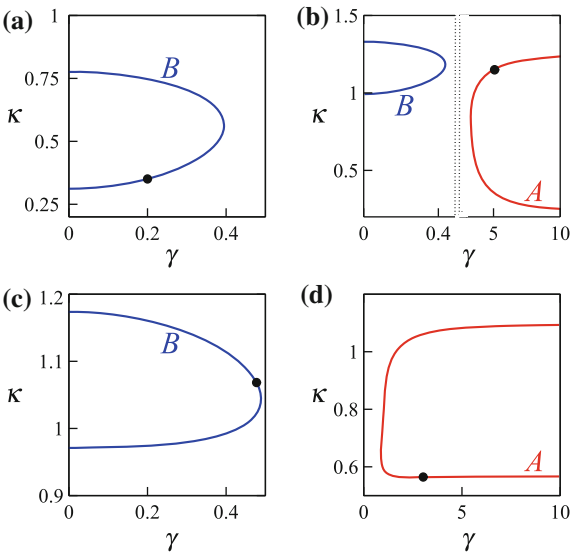

Fig. 5 "Nonlinear eigenvalues" κ versus the gain-loss coefficient γ for several sets of g and L. The *red curves* correspond to the A- and the *blue* ones to the B-modes. Solutions marked by the *black dots* are shown in Fig. 6. In these plots, $g = 1$, $L = 2.2$ (**a**); $g = 5$, $L = 2$ (**b**); $g \approx 12.12$, $L \approx 8.26$ (**c**); $g \approx 12.38$, $L \approx 9.35$ (**d**). Note a break in the horizontal axis in (**b**)

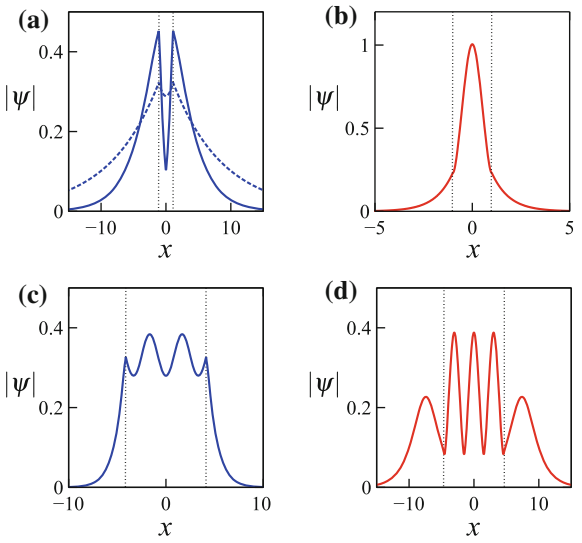

Fig. 6 *Solid curves* depict nonlinear localised modes at representative points along the $\kappa(\gamma)$ curves. (These points are marked by *black dots* in the corresponding panels of Fig. 5.) The B-modes are shown in *blue* and the A-modes in *red*. *Vertical dotted lines* indicate the positions of the potential wells. The *dashed curve* in (**a**) renders the eigenfunction of the equation (4) with $g = 0$ where L and γ are set equal to the L and γ of the nonlinear mode shown in the same panel. Note that the three-hump mode in (**d**) has four and not two local minima inside the $(-L, L)$ interval. The two lateral dips are pressed close to the wells but are nevertheless discernible by zooming in

g, T obtained by a once-off application of the map (54). A typical nonlinear mode arising along this branch is shown in Fig. 6c.

Figure 5d traces a branch of the multi-hump A-modes. Solutions on this branch have three humps and four dips situated between the wells; an example is in Fig. 6d. The starting point for the branch was suggested by the graphical analysis of the equations making up the A-system.

10 Summary and Conclusions

The double-δ well potential, where one well gains and the other one loses particles, furnishes one of the simplest Gross-Pitaevskii models employed in the studies of boson condensates. However the information on its nonlinear modes is scarce and based entirely on numerical solutions. The purpose of this contribution was to formulate an *analytical* procedure for the construction of localised nonlinear modes.

We started with the linear Schrödinger equation with the PT-symmetric double-delta well potential and provided a simple analytical classification of its bound states.

In the nonlinear situation, our procedure reduces the construction of localised modes to finding roots of a system of two simultaneous algebraic equations involving

elliptic integrals and Jacobi functions. We have classified the nonlinear modes under two broad classes: those with a maximum of $|\psi|$ at the centre and those centred on a minimum of $|\psi|$. Accordingly, there are transcendental systems of two types (referred to as the A- and B-systems). Our construction procedure is supplemented with an "identification" algorithm allowing to relate the number of crests and troughs of the nonlinear mode to the root of the transcendental system. We have established a correspondence between localised modes in systems with different distances between the wells and different nonlinearity strengths.

Our procedure has been illustrated by the construction of branches of A- and B-modes for several values of g and L.

Acknowledgments This contribution is a spin-off from the project on the jamming anomaly in PT-symmetric systems [4]; we thank Vladimir Konotop for his collaboration on the main part of the project. Nora Alexeeva's numerical assistance and Holger Cartarius' useful remarks are gratefully acknowledged. This work was supported by the NRF of South Africa (grants UID 85751, 86991, and 87814) and the FCT (Portugal) through the grants UID/FIS/00618/2013 and PTDC/FIS-OPT/1918/2012.

References

1. S. Klaiman, U. Günther, N. Moiseyev, Visualization of branch points in PT-symmetric waveguides. Phys. Rev. Lett. **101**, 080402 (2008)
2. H. Cartarius, G. Wunner, Model of a PT-symmetric Bose-Einstein condensate in a δ-function double-well potential. Phys. Rev. A **86**, 013612 (2012)
3. Z.H. Musslimani, K.G. Makris, R. El-Ganainy, D.N. Christodoulides, Optical solitons in PT periodic potentials. Phys. Rev. Lett. **100**, 030402 (2008)
4. I.V. Barashenkov, D.A. Zezyulin, V.V. Konotop, Jamming anomaly in PT-symmetric systems. Submitted for publication (2016)
5. Y.B. Gaididei, S.F. Mingaleev, P.L. Christiansen, Curvature-induced symmetry breaking in nonlinear Schrödinger models. Phys. Rev. E **62**, R53 (2000)
6. R.K. Jackson, M.I. Weinstein, Geometric analysis of bifurcation and symmetry breaking in a Gross-Pitaevskii equation. J. Stat. Phys. **116**, 881 (2004)
7. M. Znojil, V. Jakubský, Solvability and PT-symmetry in a double-well model with point interactions. J. Phys. A: Math. Gen. **38**, 5041 (2005)
8. V. Jakubský, M. Znojil, An explicitly solvable model of the spontaneous PT-symmetry breaking. Czechoslovak J. Phys. **55**, 1113 (2005)
9. H. Uncu, E. Demiralp, Bound state solutions of the Schrödinger equation for a PT-symmetric potential with Dirac delta functions. Phys. Lett. A **359**, 190 (2006)
10. H. Cartarius, D. Haag, D. Dast, G. Wunner, Nonlinear Schrödinger equation for a PT-symmetric delta-function double well. J. Phys. A: Math. Theor. **45**, 444008 (2012)